Investigating Airborne Low Frequency GPR Antenna-Ground Coupling through Modelling

D Vogt[1], M van Schoor[2]

1. CSIR, South Africa, dvogt@csir.co.za
2. CSIR, South Africa, mvschoor@csir.co.za

ABSTRACT

Ground Penetrating Radar (GPR) is often a good tool for detecting near surface structure, as it is cheap, fast and has high resolution. At lower frequencies, it is an excellent tool for detecting voids such as sinkholes, old excavations or rat-holes that pose a risk to surface infrastructure. However, in some situations, the potential risk from the voids prevents the use of GPR on the surface, and airborne application needs to be considered.

While GPR has been successfully applied from the air, the applications have usually been over ice, which is a particularly radar transparent medium. In this case, information is required about sub-surface structure in a moderately conductive environment. In order to better understand the performance of GPR, a typical resistively loaded dipole antenna with a design frequency of around 50 MHz has been modelled at various heights above the ground. The modelling was conducted using a Finite-Difference Time-Domain code that incorporates a dispersive lossy medium model.

The results show that coupling of energy into the ground is not adversely affected by raising the antenna. The antenna characteristics change, with slightly less energy being emitted at lower frequencies, but the coupling into the ground does not change. There is some change in the spreading pattern of signals in the earth that will result in small changes in the shape of the diffraction hyperbolas that are usually seen.

The modelling supports testing of an airborne system to determine whether it is capable of producing meaningful results.

Key words: Airborne Ground Penetrating Radar, void detection, Finite-Difference Time-Domain, electromagnetic modelling.

INTRODUCTION

There are a number of coal mines in the Witbank and Highveld coalfields where mining has already occurred underground by the bord and pillar method, but where it is now proposed to remove the remaining coal pillars using opencast mining methods.

There are a number of technical problems associated with reliably locating pillars in order to plan mining operations. This paper considers the problem that occurs occasionally when the void in the coal seam created by historical mining slowly propagates upwards near to the surface. The void then becomes a serious hazard to vehicles driving on the surface, and there have been accidents where vehicles have been lost.

It has been shown that Ground Penetrating Radar (GPR) can be used to identify the voids, if the ground is sufficiently resistive. However, there is understandable reluctance to employ GPR due to the danger of field crews falling into currently unidentified voids.

It has therefore been proposed to apply GPR from an airborne platform. GPR is routinely used from airborne platforms for mapping the depth of snow and ice (Vaughan et al, 1999), and is starting to be applied in other fields (Catapano et al, 2012; Krellman and Trilitzsch, 2012).

In this paper, a specific aspect of GPR antenna performance is investigated: coupling between the antenna and the ground as the antenna is raised.

METHOD

Conventional GPR antennas are designed for high-frequency, short-range penetration, and are usually constructed with shielding. The shielding ensures that the bulk of the radar energy goes into the ground, not into the air around the antenna. For the proposed

application of detecting near-surface voids in Karoo sediments, a lower frequency is likely to be required to penetrate the expected moderate conductivity.

Low frequency (less than 100 MHz) GPR antennas are typically not shielded. They are often resistively loaded to increase their bandwidth (Arcone, 1995). In this study, a resistively loaded, unshielded 2 m dipole is considered. The dipole antenna is modelled as a monopole operating against a plane of symmetry.

A 3D Finite-Difference Time-Domain (FDTD) model is used to simulate the electromagnetic propagation coming from the antenna. The code used here is described in Vogt (2000).

The model is illustrated in Figure 1. There are 20 cells in the *z* dimension, 200 cells in the *x* dimension and 300+ cells in the *y* dimension. The cells are each 5 cm × 5 cm × 5 cm. The space is either filled with a rock medium, or has an air layer above a rock layer.

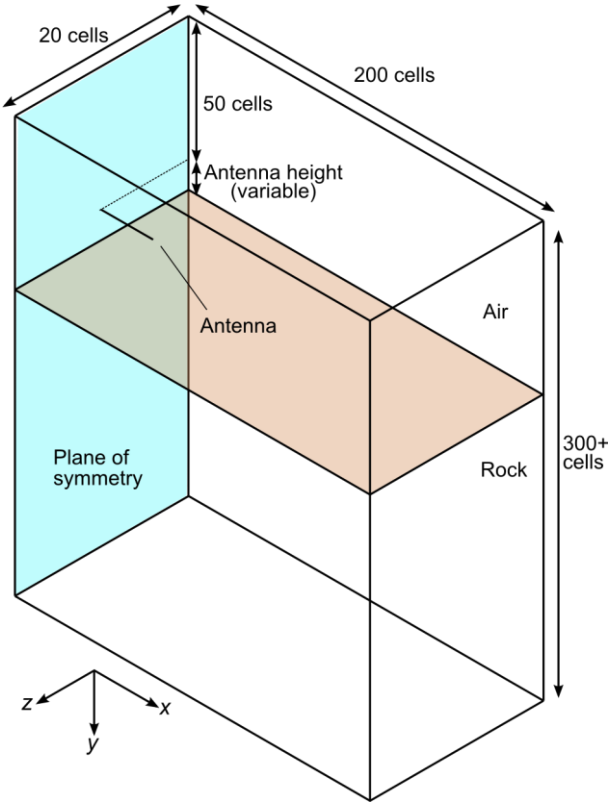

Figure 1. 3D modelling space

In an FDTD model, the electric field is modelled along each edge of each cell, while the magnetic field is modelled in the centre of each face of the cell.

To determine the effects of propagation in the rock medium, the E_x field is measured 200 cells below the surface of the rock. The bottom boundary of the model is kept at least 50 cells further away in the *y* direction. All the models have at least 300 cells vertically, but may have more if the air/rock boundary is positioned some distance from the antenna.

The antenna is placed 50 cells (or 2.5 m) below the upper boundary. If there is air in the model, the boundary between the air and the rock is placed immediately below the antenna, or at distances of 0.5 m, 1 m, 2.5 m and 5 m. All boundaries apart from the plane of symmetry are terminated using Higdon 2nd order absorbing boundaries. The plane of symmetry is a perfect electric conductor.

The models are run using two rock materials: granite and dolerite, from the catalogue in Vogt (2000). These two materials cover the range of electrical properties expected for Karoo sediments. The granite is highly resistive, while the dolerite at about the limit of conductivity that is practical for GPR use. The rock electrical properties are modelled using multiple factor Debye models valid between 1 MHz and 100 MHz.

The average properties for the two materials are:

	Granite	Dolerite
Relative permittivity	10	25
Loss tangent	0.08	0.25
Attenuation at 50 MHz	0.75 dB/m	5 dB/m
Length of run	3000 steps	8192 steps

A timestep of 8.33 ps is used. The source pulse is a bipolar Gaussian containing a nominal maximum frequency of 100 MHz, imposed on the feed point of the antenna.

The antenna is modelled as 21 segments in length. The first segment is the feed point, while all the remaining even numbered segments are thin wires. In between each thin wire, the four cells around the antenna axis are given electrical properties to model a resistor, as illustrated in Figure 2. The resistivity is determined to provide a lumped approximation of the Wu-King resistively loaded profile according to:

$$R_i(r') = \frac{R_0}{1-|r'/h|} \quad (1)$$

where R_0 is a characteristic impedance that balances performance with removal of ringing, h is the height of

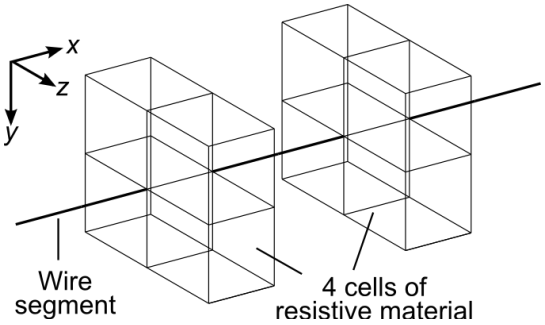

Figure 2. Modelling resistive loading (not to scale)

the monopole and *r* is the distance along the monopole (Wu and King, 1965).

For presentation purposes, an image is created of the E_x fields on the *z*=10 plane. The image is mirrored around the axis of symmetry, creating a 400 × 300 pixel image.

RESULTS

The antenna produces a field at 5 m in air having signal strength as illustrated in Figure 3. The source and antenna have a bandwidth of approximately 35 MHz to 80 MHz.

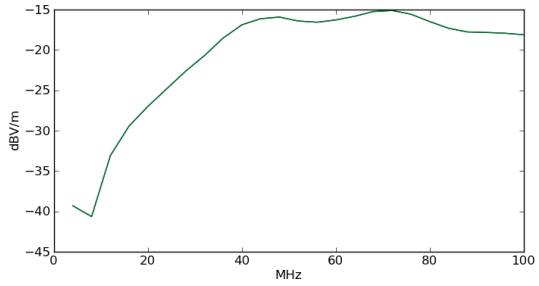

Figure 3. Signal strength 5 m from resistively loaded dipole in air.

If the E_x-field is monitored at a point 5 m below the ground, directly below the antenna, the effect of the air on antenna performance can be seen. In **Error! Reference source not found.**, a number of curves for signal strength are plotted when the rock is granite. If the antenna were completely embedded in the granite, it would produce the signal strength curve plotted in blue, at a distance of 5 m from the antenna. The bandwidth of the signal is lowered, compared to the antenna in air, because the lower velocity of propagation in rock lengthens the antenna electrically. The bandwidth now extends from roughly 20 MHz to 50 MHz.

If the antenna is raised above the surface, the effect at all four heights is similar: signal strength is not affected significantly, but there is slightly more energy at higher frequencies, because the bandwidth of the antenna increases when it is surrounded by air.

There is only a 7 dB difference in signal strength 5 m below the ground between the peak response of the antenna on the surface and the antenna 5 m in the air. The longer path and increased spreading explain much of the difference.

Similar results are achieved for the antenna over a dolerite earth: in Figure 5 there is again little difference in signal strength at 5 m depth when the antenna is on the surface or raised above it by up to 5 m. The markedly high attenuation in the dolerite is visible, as is the greater drop in signal strength as a function of frequency.

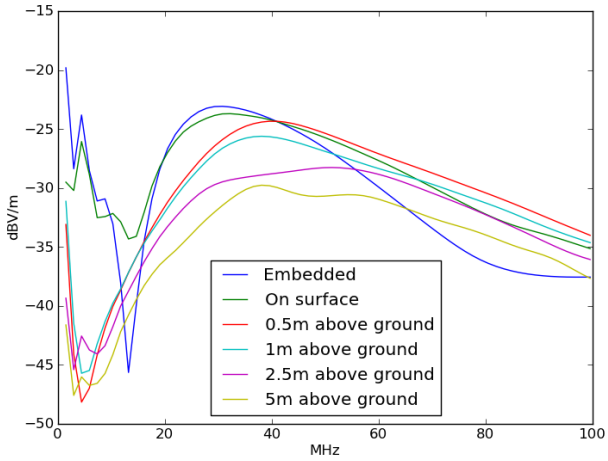

Figure 4. Signal strength 5 m below the surface of the granite, directly below the antenna.

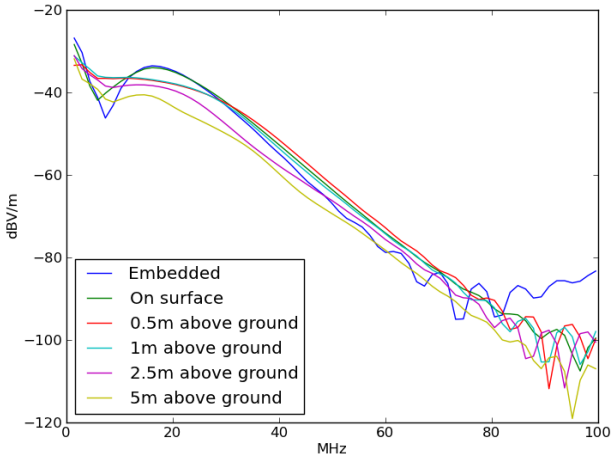

Figure 5. Signal strength 5 m below the surface of the dolerite, directly below the antenna.

In Figure 6 overleaf, the time domain performance of the antenna is captured 100 ns after the model starts, for a variety of antenna configurations and heights. At bottom right, the antenna is modelled enclosed entirely in rock. The pattern of energy going downwards in the figure closely follows the cosine pattern of a perfect dipole antenna, however there is also considerable energy radiated along the length of the antenna.

For all depths of operation, the airwave from the antenna that is refracted into the ground away from the antenna travels along the surface at a greater velocity than the propagation in the ground, causing a propagation shape that has “ears” which are flatter than the typical spherical propagation in the earth. This effect becomes more marked as the antenna is raised above the surface. Characteristic reflection hyperbolas will therefore have different shapes depending on the different heights of the antenna above the ground.

In this paper, only the height above ground of the GPR antenna is considered. In practice, the reflection from the ground surface can become a major source of

clutter, particularly if it is rough. Fu et al (2012) show that surface roughness does obscure early arrivals from the subsurface, but that deeper features may still be detected.

CONCLUSIONS

The major effect of raising a GPR antenna from the ground is to increase its frequency of operation, because the antenna is enclosed in air with a higher velocity than the rock that is normally adjacent to it. There is very little effect on the signal strength in the earth due to the change in coupling as the antenna moves away from the earth.

The modelling results presented here correspond well with experimental results presented elsewhere at this conference. At present, nothing suggests that airborne GPR antennas will not be viable for use in near-surface coal applications.

REFERENCES

Arcone, S. A., 1995. Numerical studies of the radiation patterns of resistively loaded dipoles: Journal of Applied Geophysics 33, 39-52.

Catapano, I., Crocco, L., Soldovieri, F., Lanari, R., Alberti, G., Adirosi, D., Facchinetti, C., Longo, F., Formaro, R. and Persico, R., 2012. Airborne GPR surveys via tomographic imaging: An analysis of the reconstruction capabilities: 14th International Conference on Ground Penetrating Radar (GPR), 4-8 June, 310-314.

Fu, L., Liu S. and Liu, L., 2012. Numerical simulations and analysis for airborne ground penetrating radar: 14th International Conference on Ground Penetrating Radar (GPR), 4-8 June, 200-203.

Krellmann, Y. and Triltzsch, G., 2102. HERA-G — A new helicopter GPR based on gated stepped frequency technology: 14th International Conference on Ground Penetrating Radar (GPR), 4-8 June, 156-159.

Vaughan, D. G., Corr, H. F. J., Doake, C. S. M. and Waddington, E. D., 1999. Distortions of isochronous layers in ice revealed by ground-pentrating radar: Nature, 398, March, 323-326.

Vogt, D., 2000. The modelling and design of radio tomography antennas: PhD Thesis, University of York.

Wu, T. T. and King, R. W. P., 1965, The cylindrical antenna with nonreflecting resistive loading: IEEE Transactions on Antennas and Propagation 13(3), 369-373 correction 13(6), 998.

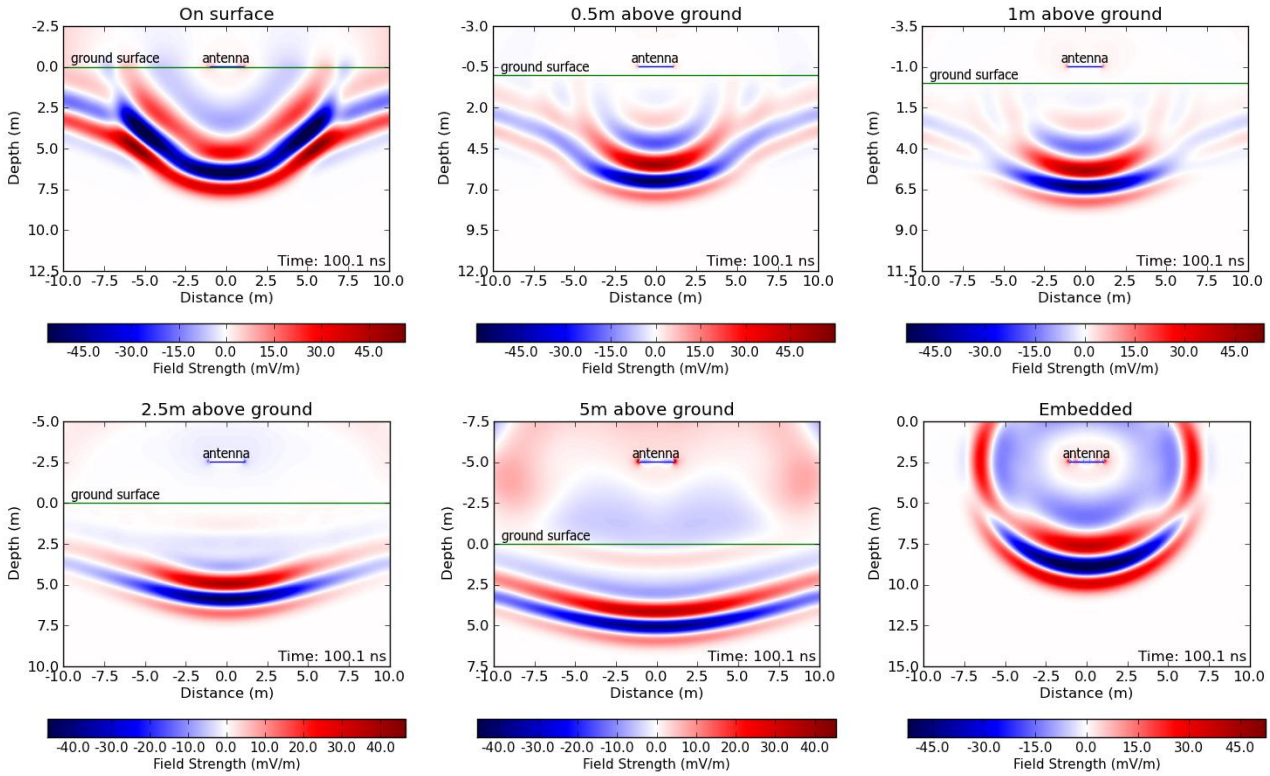

Figure 6. Time domain snapshots of the signal propagation from an antenna at various heights above the surface of granite. The E_x signal strength in the model is plotted.